Timeresolved infrared spectral photography: Study of laserinitiated explosions in HN3

Ph. Avouris, D. S. Bethune, J. R. Lankard, J. A. Ors, and P. P. Sorokin

Citation: The Journal of Chemical Physics **74**, 2304 (1981); doi: 10.1063/1.441347
View online: http://dx.doi.org/10.1063/1.441347
View Table of Contents: http://scitation.aip.org/content/aip/journal/jcp/74/4?ver=pdfcov
Published by the AIP Publishing

Time-resolved infrared spectral photography: Study of laser-initiated explosions in HN_3

Ph. Avouris, D. S. Bethune,[a] J. R. Lankard,[a] J. A. Ors,[b] and P. P. Sorokin[a]

IBM Thomas J. Watson Research Center, Yorktown Heights, New York 10598
(Received 18 August 1980; accepted 21 October 1980)

Recent improvements in the technique of time-resolved infrared spectral photography (TRISP) are described. With this technique CO_2 laser-induced thermal explosions of gas phase HN_3/DN_3 mixtures were investigated. HCl gas added to the mixtures was utilized to probe the transient temperature of the reaction. An induction period and a phase of rapid energy release were clearly identified and characterized both with respect to temperature and utilization of reactant material.

I. INTRODUCTION

Time-resolved spectroscopic techniques can be used to probe the dynamics of chemical events and provide information regarding the distribution of energy among internal states of reaction products. In addition, the structures and energy levels of highly transient chemical intermediates such as free radicals can be obtained using these techniques.

The powerful and widely used time-resolved electronic absorption and emission techniques[1–3] have their own limitations. Since only relatively few molecules possess emission spectra, time-resolved emission techniques have limited generality. For the determination of internal energy distributions by electronic absorption or emission techniques, one needs additional parameters, such as Franck–Condon factors, which are largely unknown, except for simple molecules. Of more importance, it is very difficult to obtain molecular structural information for unknown chemical intermediates (except for very simple fragments) by measuring electronic absorption or emission spectra.

Vibrational spectroscopy, however, is an indispensable technique for "fingerprinting" molecular structures.[4] Infrared (IR) and Raman frequencies can be used in many cases to uniquely characterize the chemical structure of a molecule. Furthermore, with IR or Raman techniques the determination of the vibrational and rotational populations of product molecules requires only knowledge of ground state properties, which are generally much better known than those of excited electronic states. It is highly desirable, therefore, to be able to record transient broadband IR absorption (and Raman) spectra.

We have recently developed[5,6] a technique for taking single-shot time-resolved IR absorption spectra (TRISP). Briefly, this technique works as follows: Light from a broadband dye laser is converted into a pulsed infrared continuum beam by stimulated broadband electronic Raman scattering in an alkali metal (e.g., Rb) vapor. This infrared continuum beam is made to probe the absorption of the sample, and is then upconverted back to the visible region by a four-wave mixing process in a second metal vapor cell. The dispersed upconverted light, which is easily photographed, contains an absorption spectrum that is a proportional replica of the IR absorption spectrum. In the present paper we describe the current implementation of this technique, which incorporates several improvements over the previously reported version.[6] We also describe results obtained using TRISP to investigate the CO_2 laser-induced thermal explosion of hydrazoic acid (HN_3).

As has been recently demonstrated,[6–9] lasers can be utilized to initiate chemical explosions in a fast, homogeneous fashion, free of wall effects. The fast laser initiation makes these explosions particularly amenable to time-resolved spectroscopic studies.

The thermal decomposition of HN_3, i.e.,

$$2HN_3 \rightarrow H_2 + 3N_2, \quad \Delta H = -72 \text{ kcal/mol}, \tag{1}$$

is a highly exothermic reaction and, under appropriate conditions, can lead to a thermal explosion. In a study of the UV spectrum of products resulting from flash photolysis of HN_3, Thrush[10] in 1956 observed that explosions tended to occur above certain levels of input flash energy. These explosions were accompanied by characteristic changes in the UV absorption spectrum, viz., the sudden appearance of the 3360 Å $^3\Pi \leftarrow {}^3\Sigma$ NH band system and the sudden disappearance of a band system at 2700 Å which was produced by the photolysis pulse. The 2700 Å system, correctly attributed to N_3 by Thrush,[10] was later analyzed in greater detail.[11] Earlier spectroscopic work had focused on the luminescence emitted by propagating, spark-initiated explosions in HN_3. Pannetier and Gaydon[12] remarked that this luminescence was rather weak, and they were able to discern clearly only the (0, 0) and (1, 1) $^3\Pi \rightarrow {}^3\Sigma$ bands of NH. Flames in HN_3 diluted with various inert gases have also been studied to obtain burning velocities and quenching diameters for purposes of comparison with various theories of propagating explosions.[13]

There is reason to believe that the molecular nitrogen produced according to Eq. (1) will be highly vibrationally excited. This notion was used about 10 years ago by two groups[14,15] to obtain CO_2 laser action. For this purpose, mixtures of HN_3 and CO_2 were exploded by long flash photolysis pulses.

In more recent years, the emphasis in work dealing

[a]Supported in part by the U. S. Army Research Office.
[b]Present address: Western Electric, Engineering Research Center, Box 900, Princeton, New Jersey 08540.

 0021-9606/81/042304-09$01.00

with the decomposition of HN_3 has switched to spectroscopic studies of the primary steps in the photolysis of this compound at low pressures. Such studies involve laser photolysis by both UV[16] and IR[17] pulses. It appears that in both cases the primary dissociation process is

$$HN_3 + (\hbar\omega_{UV} \text{ or } n\hbar\omega_{IR}) \rightarrow NH^*(^1\Delta) + N_2 \ . \quad (2)$$

A subsequent fast chemiluminescent reaction was also identified,[16,17] namely,

$$NH^*(^1\Delta) + HN_3 \rightarrow NH_2^*(^2A_1) + N_3 \ . \quad (3)$$

Reactions that follow initial steps (2) and (3) have been proposed, however, with very little supporting spectroscopic evidence. This is particularly true in the case of HN_3 explosions.

As stated above, we succeeded in producing with a CO_2 laser beam fast thermal explosions in mixtures of HN_3 and DN_3. DN_3 was used because it is a much stronger absorber at the CO_2 laser wavelength. The time scale of these explosions was established by TRISP and by traditional photoelectric techniques. We also investigated exploding mixtures of HN_3/DN_3 and HCl, utilizing HCl as an internal thermometer to probe the transient temperature of the explosion. This was accomplished by monitoring with TRISP the rotational temperature of HCl as a function of time. On the basis of these measurements, we speculate on the nature of the chemical processes responsible for the thermal explosion. The HN_3 explosion studies reported here demonstrate some of the present capabilities of TRISP. Improvements which should enhance these capabilities are also briefly discussed.

II. BASIS OF TRISP

Time-resolved infrared spectral photography is a method for recording broadband (~ 1000 cm^{-1}) IR absorption spectra with moderate resolution (~ 0.5 cm^{-1}) in short times (~ 10 ns). This is accomplished by (1) generating a short pulse of collimated, broadband, IR radiation, (2) passing the IR through a sample so that the emerging beam has its spectral envelope modulated by the sample absorption, and (3) upconverting the IR using a nonlinear optical process to give a visible light pulse whose spectral envelope is proportional to the IR spectral envelope. A standard visible light spectrograph is used to disperse and photographically record the entire upconverted spectrum simultaneously.

The nonlinear optical processes underlying the IR generation and upconversion processes are diagrammed in Fig. 1. On the left side of the figure is a schematic level diagram for Rb atoms, with the stimulated electronic Raman scattering (SERS) process responsible for the IR generation indicated by the arrows. When the SERS threshold is exceeded, broadband visible continuum light ν_C is absorbed, broadband infrared (Stokes) radiation ν_{IR} is emitted, while Rb atoms are simultaneously excited from the 5s to the 6s state. For each visible frequency there is produced a corresponding infrared frequency shifted by $\Delta\nu_R$, the frequency associated with the 5s–6s transition. Thus, the broadband

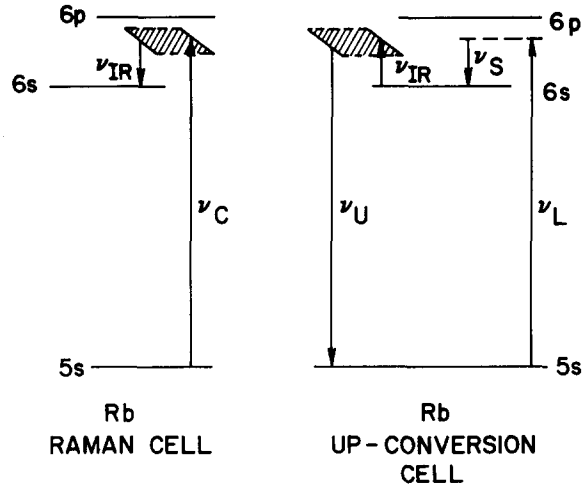

FIG. 1. Level diagrams for the SERS infrared generation and four-wave parametric upconversion processes in Rb vapor; ν_C and ν_{IR}—broadband visible and IR continua, respectively; ν_L and ν_S—narrow-band visible laser and its Raman Stokes IR beam, respectively; ν_U—upconverted visible beam.

visible spectrum is transformed to an infrared spectrum with essentially the same spectral bandwidth. Because the infrared radiation experiences gain along the path pumped by the visible beam, the infrared emerges in a well-collimated beam, essentially collinear with the pump light. With visible pulse energies of ~ 10 mJ, approximately 100 μJ of infrared is generated.

If the infrared spectral density is labeled $I_{IR}(\nu_{IR})$, the spectrum emerging from the sample is given by

$$I_{IR}^*(\nu_{IR}) = I_{IR}(\nu_{IR}) \exp[-\alpha(\nu_{IR})l] \ , \quad (4)$$

where α is the infrared absorption coefficient and l is the sample length. The interaction of the probe beam with the sample is thus ordinary linear absorption. The infrared energy per bandwidth is low enough (~ 10^{-7} J/cm^{-1}) so that nonlinear effects (e.g., multiphoton absorption or saturation of IR transitions) are expected to be negligible, even if the probe beam is weakly focused.

The upconversion process is diagrammed on the right-hand side of Fig. 1. In this process a narrow-band laser (with frequency ν_L) drives SERS in a second Rb vapor cell, generating a narrow-band Stokes infrared beam (with frequency ν_S). This stimulated scattering process produces an electronic oscillation of the atoms at frequency $\Delta\nu_R = (\nu_L - \nu_S)$. When the infrared light passes through this excited medium, a polarization component at frequency $\nu_U = (\Delta\nu_R + \nu_{IR})$ is parametrically produced for each infrared frequency. The component can be written

$$\mathbf{P}(\nu_{IR} + \Delta\nu_R) = F\mathbf{E}_{IR}(\nu_{IR}) \ , \quad (5)$$

where F is a function of frequency and spatial position and $\mathbf{E}_{IR}(\nu_{IR})$ is the ν_{IR} frequency component of the infrared electric field. The intensity of the corresponding spectral component of the generated upconverted light is proportional to the squared magnitude of this polarization component, so that $I_U(\nu_{IR} + \Delta\nu_R) \propto I_{IR}^*(\nu_{IR})$. Since the upconverted spectrum is linearly proportional

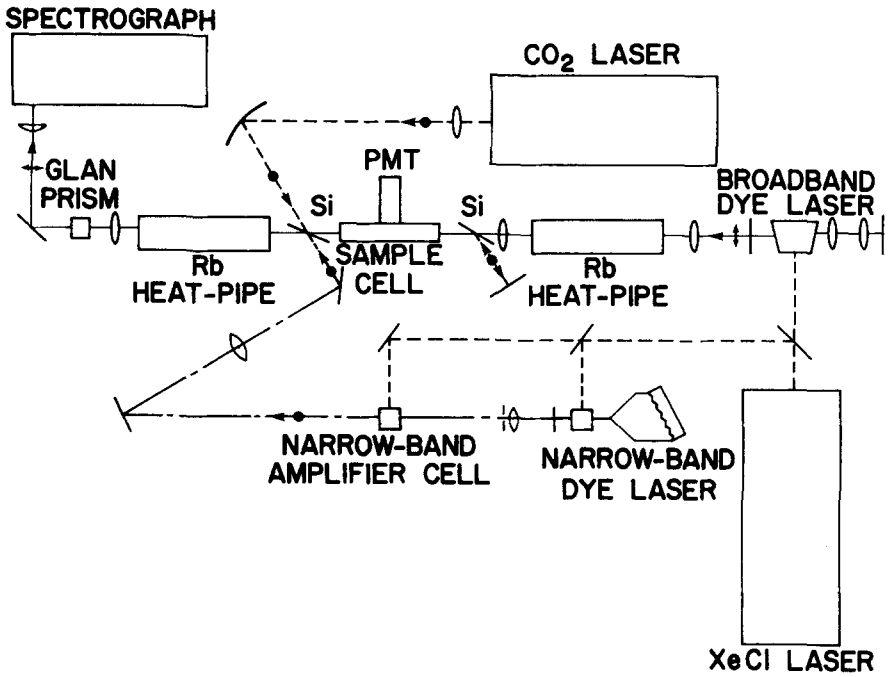

Fig. 2. Diagram of experimental apparatus. Details are given in the text.

to the infrared spectrum, the absorption coefficient can be recovered from

$$\alpha(\nu_{IR}) = l^{-1} \ln[I_0/I_U(\nu_{IR} + \Delta\nu_R)] \ , \tag{6}$$

where $I_0(\nu_{IR} + \Delta\nu_R)$ is a reference upconverted spectrum taken with the sample removed. Ideally, one would simultaneously record the sample and reference spectra, and it is possible to do this by splitting the infrared beam before the sample and upconverting the two portions separately. However, we have so far recorded the two spectra sequentially.

The attainable spectral resolution is limited in two ways. First, the visible spectrometer always limits the resolution, even though the excellent collimation of the upconverted beam allows it to be focused onto a fine slit with little loss of light. A more fundamental limitation is imposed by the finite bandwidth of the electronic Raman oscillation, as revealed by the bandwidth[18] of infrared Stokes beams generated with extremely monochromatic pump beams. For alkalis, under typical conditions, this width is measured to be $\sim 0.5\ cm^{-1}$.[18]

III. EXPERIMENTAL

The present TRISP apparatus, diagrammed in Fig. 2, is considerably modified from that described in Ref. 6. The three-stage visible continuum generator used in Ref. 6 has been replaced with a single broadband dye laser, transversely pumped with 75% of the output from a 150 mJ/pulse XeCl excimer laser (Lumonics 260-2). The remaining 25% of the excimer laser output pumps a narrow-band dye laser (actually, an oscillator–amplifier combination using a solution of bis-MSB in *p*-dioxane). This narrow-band dye laser beam, with ~2 mJ/pulse energy, drives the upconverter. A 10^{-3} M solution of Coumarin 440 in ethanol was used in the broadband dye laser. The output energies of this laser were in the 10–20 mJ range. Relatively high output energies are necessary to exceed the broadband Raman threshold in Rb vapor with a Coumarin 440 dye laser beam since the latter lases at wavelengths fairly far removed from the Rb 6*p* resonance lines. The advantage of this particular combination is that the entire spectral region extending from 2500 to 3600 cm^{-1} can be probed with each shot. This region includes the ν_1 (NH stretch) band of HN_3.

As was the case with our earlier TRISP apparatus,[6] single-shot spectra display a random spectral noise, although this effect is considerably reduced in the present setup, for reasons which are still unclear to us. Since this spectral noise tends to average out, we routinely superimpose 10 to 15 shots per exposure, even though, in the case of explosions, this entails as many fillings of the sample cell. The number of shots per exposure are indicated in each figure.

The CO_2 TEA laser used to initiate explosions in these experiments is a Tachisto TAC II laser used with a broadband totally reflecting rear mirror. The multimode output occurs at 10.6 μm, near the center of the strong ν_4 hydrogen bending mode of DN_3.[19] The output pulse energy was approximately 1 J.

The vertically polarized laser beam passed through a 2 m BaF_2 lens, then reflected off a 4 m radius mirror onto a thin (≈ 15 mil thick) Si reflecting wafer. Both wafer surfaces were polished and were parallel to within a few arc seconds. The angle of incidence of the CO_2 laser beam was chosen to be near Brewster's angle for Si. With subsequent fine tuning of the angle of incidence, constructive interference of the 10.6 μm beams reflected from the two surfaces of the Si wafer was realized, resulting in maximum reflected beam intensity. Virtually all of the CO_2 laser beam energy could be directed in this way into a 25 cm long, 1 cm diameter Pyrex sam-

ple cell equipped with NaCl end windows. With the 2 m lens–4 m mirror combination, the CO_2 laser beam gradually focused down to a spot size ~ 8 mm in diameter, with a long waist extending through the sample cell. In an attempt to achieve homogeneous excitation of the gas, the nonabsorbed 10.6 μm beam was reflected back through the sample cell with the aid of a second polished Si wafer and an additional reflecting mirror. As Fig. 2 shows, the two Si wafers serve not only to couple the CO_2 beam into the sample—they also perform essential filtering and beam combining functions in the TRISP apparatus. To monitor the time history of the light emitted by each explosion, a 1P28 (S-5) photomultiplier tube, placed at right angles to the sample cell, equidistant from either end, was employed.

Gaseous mixtures of HN_3 and DN_3 were prepared by adding excess 1:1 mixtures of stearic acid and monodeuterostearic acid to sodium azide and heating to about 110 °C under vacuum. As soon as generation of HN_3 and DN_3 commenced, the pumping channel was closed, and the slowly evolving gas was collected in 2 ℓ glass bottles at pressures of up to 100 Torr. The monodeuterostearic acid was prepared according to the same method described in Ref. 19. However, since we deliberately sought to generate mixtures of HN_3 and DN_3, there was no need for us to separate these gases by distillation methods, well known to be extremely hazardous with these compounds.

IV. RESULTS

A. Laser-initiated explosions in 1 : 1 HN_3, DN_3 mixtures

1. Phenomenology

With 20–50 Torr of a 1:1 mixture of HN_3 and DN_3 introduced into the sample cell, firing of the CO_2 laser produces an explosion of the gas evidenced by an orange flash. For an initial total gas pressure of 34 Torr, the response of the 1P28 photomultiplier tube at early times is as shown in Fig. 3. It is seen that this portion of the light emitted by the explosion rise to a peak in a time of the order of 1 μs, after a relatively short induction period lasting 1 or 2 μs. Subsequent irregular oscillations occur as this light pulse decays with a time constant on the order of 10 μs. Because of the low intensity of this light, it was not possible to resolve it spectrally with a gated optical multichannel analyzer (OMA).

At times greater than about 30 μs a much stronger light emission occurs, slowly reaching a maximum intensity in about 250 μs. Using the OMA in an integrating mode, we spectrally resolved this emission and found it to comprise emissions of impurities ablated from the Pyrex cell walls and NaCl windows. Present were the Na (589 nm) and Li(670 nm) resonance lines and bands characteristic of CaOH.[20] It is concluded that the weak light pulse seen at early times represents the intrinsic light emission from the explosion, and that the later strong emission is produced thermally.

2. TRISP probe of 1 : 1 HN_3/DN_3 explosions

A spectral photograph of the infrared absorption of HN_3 in the vicinity of the ν_1 band (NH stretch), taken with the method of TRISP, and the corresponding densitometer trace are shown in Fig. 4.

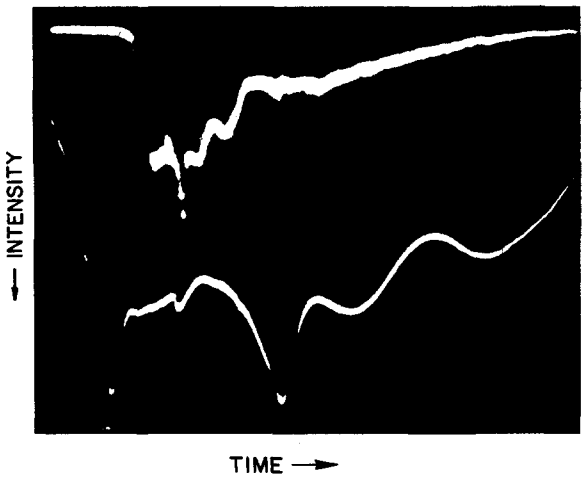

FIG. 3. Scope trace of photomultiplier signal observed during explosion with no HCl added. Upper trace: 5 μs/div., 20 mV/div. The CO_2 laser fires ~3 μs after the trace begins. Lower trace: same pulse as shown in upper trace with time scale expanded to 1 μs/div. and vertical scale 10 mV/div.

The third and fourth harmonics of ν_1 at 9547.31 and 12412.19 cm^{-1} have previously been studied photographically under high dispersion.[21,22] However, to our knowledge, not even medium resolution studies of the $\nu_1(HN_3)$ fundamental exist in the published literature.

Some of the line-like ${}^PQ_K$, ${}^QQ_K$, and ${}^RQ_K$ branches are labeled in Fig. 4. The nomenclature used here is standard: The large letter describes the behavior of J in the transition, the left-hand superscript describes the behavior of K, and the right-hand subscript gives the value of K''. At somewhat higher vapor densities than that corresponding to Fig. 4, ${}^PQ_K$ branches up to $K=6$ and ${}^RQ_K$ branches up to $K=5$ are observed. We have checked that the separations ${}^RQ_K-{}^PQ_{K+2}$ and ${}^QQ_K-{}^PQ_{K+1}={}^RQ_K-{}^QQ_{K+1}$, determined from Fig. 4, agree well with values obtained by substitution of tabulated HN_3 ground state data[22] into simple algebraic functions given in Ref. 21. What is observed in Fig. 4 that cannot be deduced from either ground state or overtone data is a pronounced K-type doubling of the $v'=1$, $K'=1$ state. This is manifest as a ~1–2 cm^{-1} splitting of the following branches: ${}^PQ_2$, ${}^QQ_1$, and ${}^RQ_0$, while all other ${}^PQ_K$, ${}^QQ_K$, and ${}^RQ_K$ branch splittings in Fig. 4 are too small to be resolved.

The envelopes of the various ${}^QR_K$ and ${}^QP_K$ branches overlap to form the double peaked, broad absorption feature seen in Fig. 4, although finely spaced components of several ${}^QR_K$ and ${}^QP_K$ branches are also evident.

The extra lines in Fig. 4 are Rb (and Cs impurity) lines arising from the TRISP metal vapor cells. They serve as useful IR frequency calibration points.

Figure 5 shows densitometer traces of TRISP spectra probing 34 Torr of a 1:1 HN_3/DN_3 mixture during an explosion. A spectral region that spans the ν_1 band of HN_3 is again shown. For the middle trace of Fig. 5, the TRISP apparatus was triggered by the intrinsic explosion light pulse itself; the XeCl laser fired approxi-

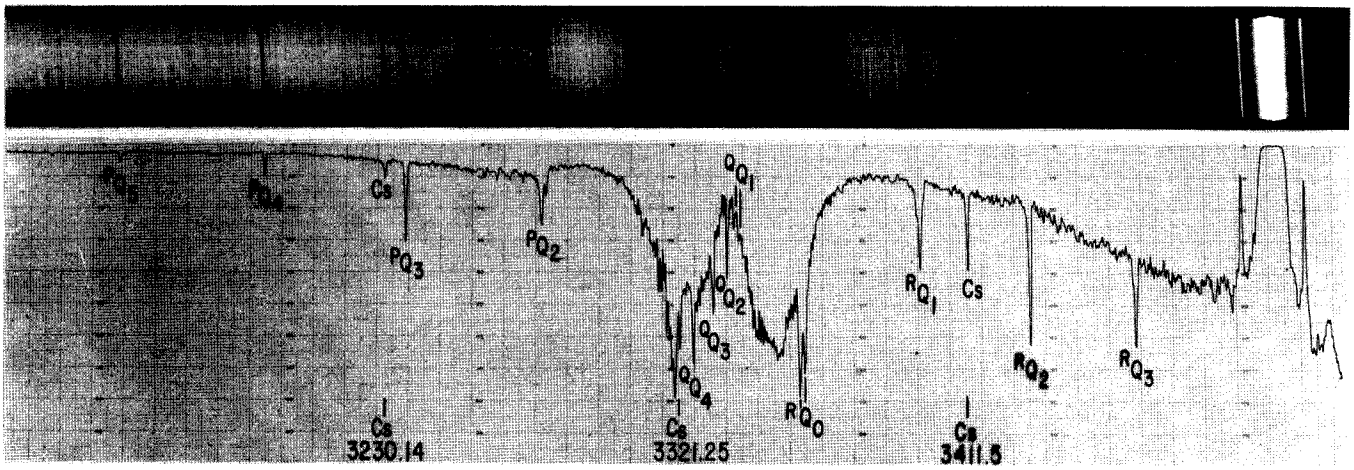

FIG. 4. Upconverted TRISP spectrum (15 shots; superimposed) showing absorption of NH_3 in the 3 μm ν_1 band (~ 17 Torr, 25 cm path). Upper: direct print from spectrographic plate (type 103-0). Lower: densitometer trace from plate. Cs reference line frequencies are given in wave numbers (cm^{-1}).

mately 2 μs after the start of the latter. In the middle trace of Fig. 5 some HN_3 is still apparent, but its absorption bands are very much broadened. The prominent, sharp bands $^RQ_1$, $^RQ_2$, $^RQ_3$, $^PQ_2$, $^PQ_3$, and $^PQ_4$, seen in Fig. 4, are all almost entirely obliterated in the middle trace of Fig. 5; only weak remnants of some of them remain. The interpretation of the broadened HN_3 bands seen in this figure is best given in conjunction with the results described in Sec. IV B.

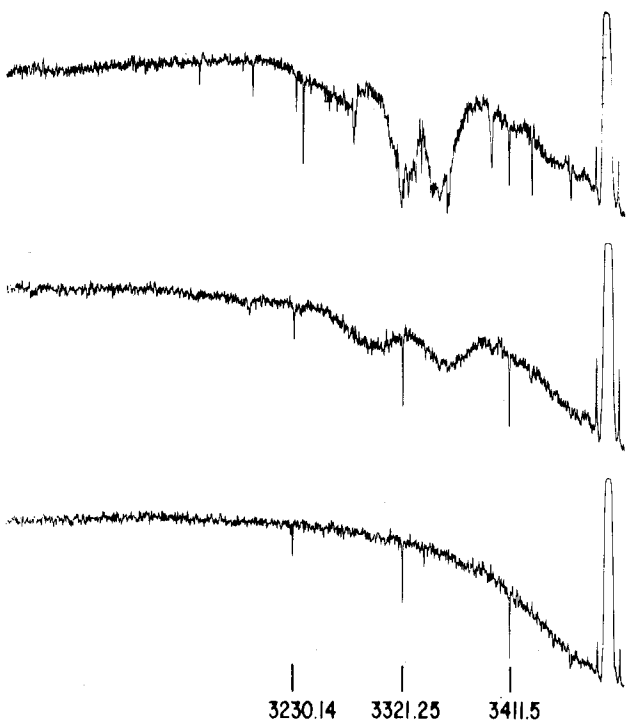

FIG. 5. TRISP spectra of NH_3 3 μm band: before explosion, 2 μs after the beginning of the explosion, and after the cell has cooled back to room temperature. No HCl was added here. The Cs calibration line frequencies are given in cm^{-1}. Number of shots/exposure: 10, 15, and 10.

3. UV probe–NH spectrum

An effort was made to photograph the absorption spectrum of the exploding gas in portions of the visible and UV spectral regions. For these measurements dye continua beams were double passed through the sample cell, using the two Si wafers and retroflector shown in Fig. 2.

A near UV absorption probe conducted with a 10 ns broadband *p*-terphenyl in EtOH laser revealed the presence of $^3\Pi \leftarrow {}^3\Sigma$ absorption bands of NH and ND early in the course of the explosion. The characteristic absorption features first appeared ~ 3 μs after the CO_2 pulse, and then persisted for several tens of microseconds, vanishing after 50 μs or so. The most notable spectral features that were seen in the single-shot exposures were the line-like maxima of the Q branches of the (0, 0) bands of NH and ND at about 336.0 and 335.7 nm, respectively. Considerably weaker were the (1, 1) bands of NH and ND at 337.0 and 336.4 nm, respectively. P branch structure of the 0–0 band of NH was evident as a series of close triplets at longer wavelengths. Lines corresponding to absorption from occupied rotational levels with N as high as 21 were seen, corresponding to a rotational energy of ~ 7550 cm^{-1}. Following Ref. 23, we can make a rough estimate of the concentration of NH radicals in the system by assuming the value $\epsilon = 40\,000$ for the extinction coefficient of the 336.0 nm absorption band. With an optical pathlength of 50 cm, the approximate measured $(OD)_0$ of 1.0 implies an NH concentration of ~ 10^{-2} Torr. This concentration is too low to be detected in a single pass with our TRISP apparatus.

Our observation of the sudden appearance of rotationally excited $^3\Sigma$ NH (and ND) in laser-initiated explosions of mixtures of HN_3 and DN_3 is consistent with the observations of Thrush on flash photolysis induced explosions.[10] Thus, absorption by $^3\Sigma$ NH is evidently a general spectral signature of the explosive decomposition of HN_3 (but not of the photolytic decomposition[16]). We were unable to probe the 270 nm region to look for N_3. A probe with a Rhodamine 6G continuum beam (580–603

nm) revealed only the two Na resonance lines (589.6 and 589.0 nm) in absorption. These appeared with moderate strength, starting ~ 30 μs after the CO_2 pulse and persisting for times as long as 300 μs. It is noteworthy that no absorption bands attributable to $^2A_1 - {}^2B_1$ NH_2, ND_2, or NHD transitions were seen. These would, in part, have occurred in the Rhodamine 6G continuum range.

B. Explosions of 1 : 1 HN_3/DN_3 mixtures with added HCl

In our previous study[6] of laser induced explosions it was shown that TRISP could be used to determine the transient temperature of a reaction by monitoring rotational band broadening. Specifically, the separation between the maxima of the P and R branches of the ν_1 band of thermally exploding CH_3NC was followed in time, leading to a determination of the time-varying temperature for the dwindling population of molecules not yet isomerized. A more general approach would be to probe the temperature of a reaction by observing the spectra of stable molecules which are present in the gas mixture during the entire reaction. As a step in this direction, we have studied explosions in mixtures of HN_3/DN_3 and HCl. HCl is a thermally stable molecule, and our experiments show that it persists during the entire reaction. In addition, HCl has a simple IR spectrum in a convenient region. Although HCl is not significantly consumed during the reaction, transient interactions with reactive intermediates of the explosion may occur.

The time variation of the PM response to the explosion light is shown in Fig. 6 for the case that 46 Torr of HCl is added to 34 Torr of 1 : 1 HN_3/DN_3. By comparison with Fig. 3, one sees that with HCl added there is a very much longer induction period before the main pulse occurs. In Fig. 6 this is roughly 275 μs, compared with 1 or 2 μs for the case of Fig. 3. On the other hand, the apparent pulse width with HCl added is only ~ 1.5 times the value with no HCl, and the ratio

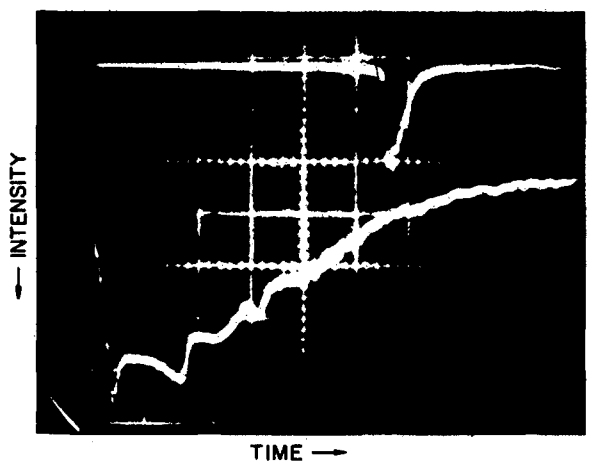

FIG. 6. Scope trace of the photomultiplier signal observed with 46 Torr of HCl added to sample. Upper trace: 50 μs/div. 20 mV/div. The CO_2 laser fires ~ 3 μs after the trace begins. Lower trace: same pulse as shown in upper trace with time scale expanded to 5 μs/div. and vertical scale 10 mV/div.

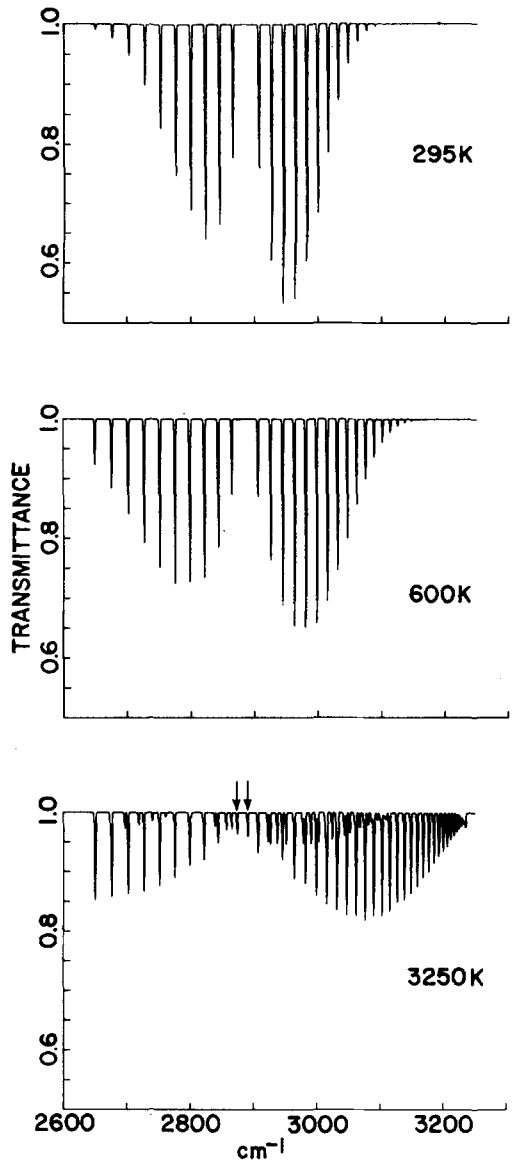

FIG. 7. Calculated IR absorption spectrum of HCl gas at various temperatures. Arrows indicate two R-branch transitions of the $v = 2 \leftarrow v = 1$ hot band.

of pulse rise times is also of this order. As will be seen below, TRISP spectra clearly show that the sharply rising light pulse detected by the PM in the case of HCl-doped mixtures is time coincident with the main energy releasing step in the explosion.

HCl is a simple diatomic whose absorption spectrum as a function of temperature is easily calculated (Fig. 7). In Fig. 8 are shown densitometer traces of TRISP spectra taken at various times falling within the long induction period that characterizes explosions of HCl and 1 : 1 HN_3/DN_3 mixtures. In the top trace a mixture (46 Torr HCl and 34 Torr 1 : 1 HN_3/DN_3) is probed before the explosion. One observes, in addition to the ν_1 band of HN_3, the well known P and R branches of HCl, comprising isotopically split (HCl^{35}, HCl^{37}) rotational lines. The next three traces show the absorption of the same mixture probed 50, 140, and 200 μs, respectively, after the CO_2 pulse has initiated the explosion. These

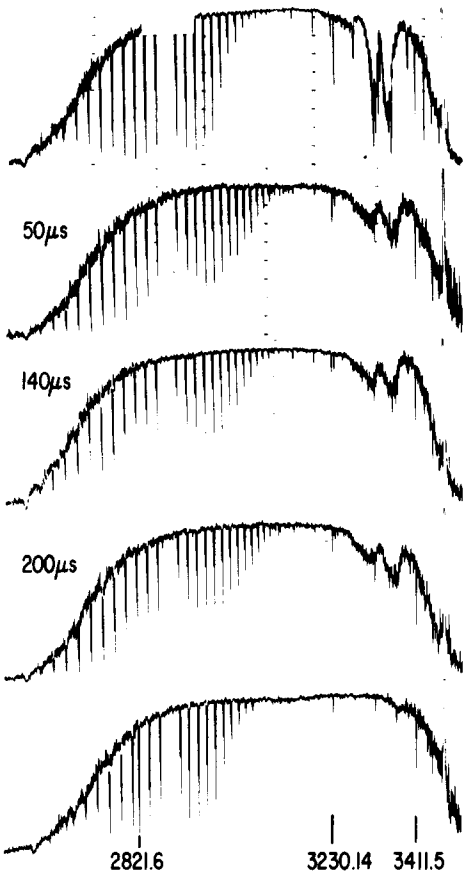

FIG. 8. TRISP spectra of $NH_3/DN_3/HCl$ (17/17/46 Torr) mixture taken before the CO_2 pulse, at indicated times during the induction period (after the CO_2 pulse but before explosion), and after the cell has cooled following explosion. One HCl line (on left) and two Cs lines (on right) are indicated, with frequencies given in cm^{-1}. Each spectrum represents 15 superimposed shots.

times were chosen to span the entire induction period, which was about 250 μs in this case; the sharply rising light pulse detected by the PM occurred soon after the last active time probe in Fig. 8. The bottom trace in Fig. 8 probes the absorption of the mixture long after the explosion has occurred and the gaseous products have cooled. A small amount of HCl appears to have been consumed.

From Fig. 8 we conclude (1) the temperature of the exploding mixture remains constant at ≈ 600 K during the entire induction period, and (2) very little HN_3 is consumed during this time. The value of the temperature (600 K) was estimated by comparing the full width at half peak amplitude of the HCl R branch envelope with the corresponding quantity in computer generated plots, such as those shown in Fig. 7. We estimate an accuracy of ± 50 K for this determination. The 300 K jump in temperature occurring at the start of the induction period represents thermal heating of the gaseous sample by the CO_2 laser pulse.

Spectra of explosions taken at various time intervals from the start of the main explosion light pulse are shown in Fig. 9. For Fig. 9, as for Fig. 5, the variable delay pulse generator that fires the TRISP apparatus was itself triggered by the leading edge of the PM response to the main explosion light pulse.

One sees from Fig. 9 that the light pulse detected by the PM is, indeed, time coincident with the main energy releasing step of the explosion. A crude estimate of the maximum transient temperature reached in Fig. 9 shows it to be in excess of 3000 K. Note the appearance in Fig. 9 of a limiting band head in the HCl R branch resulting from thermal occupation of J'' values in excess of $J'' = 21$. This is seen more clearly in Fig. 10, which contains an expanded view of the HCl bands in the same sequence shown in Fig. 9. Note the appearance of $v = 1$ to $v = 2$ vibrational transitions in Figs. 9 and 10. Two members of the R branch for this hot band sequence are marked by arrows in Fig. 10. These correspond to the arrow shown in Fig. 7.

From Fig. 9 it is apparent that for some time after the start of the main explosion light pulse, the IR probe beam senses a dwindling portion of gas that has been heated by the CO_2 laser, but that has not yet exploded. Despite efforts made to insure homogeneous excitation by the CO_2 laser beam, the explosion is evidently not totally homogeneous. This same interpretation must clearly also apply to Fig. 5.

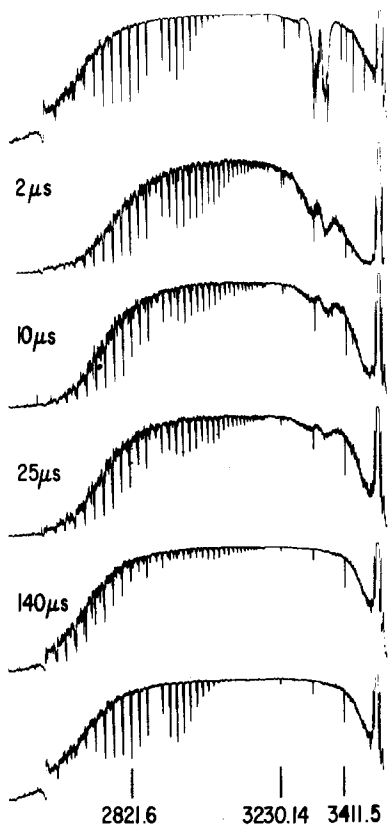

FIG. 9. TRISP spectra taken with the same sample as in Fig. 8: before the CO_2 pulse, at indicated times after the beginning of the explosion light pulse, and after the cell has cooled back to room temperature. Reference lines as in Fig. 8. Shots/exposure: 20, 20, 20, 15, 20, and 20.

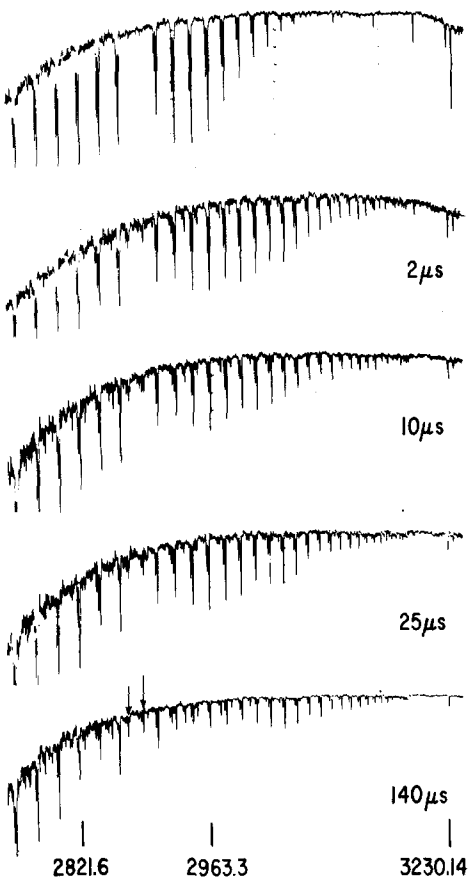

FIG. 10. Detail of HCl spectra made from same plates as in Fig. 9. Arrows indicate two R-branch transitions of the $v=2 \leftarrow v=1$ hot band. Two HCl lines (on left) and one Cs line (on right) are indicated for reference, with frequencies in cm^{-1}.

V. DISCUSSION

We assume that during the long induction period observed in Fig. 6, the CO_2 laser heated mixture undergoes slow quasi-isothermal decomposition according to Eqs. (2) and (3), resulting in a buildup of N_3 radicals. An additional reaction that could be effective during this period is one frequently mentioned in connection with HN_3 chemistry:

$$NH_2(^2B_1 \text{ or } {}^2A_1) + HN_3 \rightarrow NH_3 + N_3 \ . \tag{7}$$

When a critical density of N_3 radicals is reached, an explosive acceleration of the reaction could be provided by their exothermic recombination:

$$2N_3 \rightarrow 3N_2, \quad \Delta H = -210 \text{ kcal/mol} \ . \tag{8}$$

This could account for the main energy releasing step of the explosion, signaled by the intrinsic light pulse. The critical N_3 density for Reaction (8) to become important could well be a few orders of magnitude smaller than the starting density of HN_3, which explains why very little amounts of the latter seems to be consumed during the entire induction period. The deduced induction period temperature of 600 K for the particular HCl doped mixture we have chosen to study is close to a threshold temperature for explosion for gas of that particular composition and pressure, as evidenced by the failure of the mixture to explode if the CO_2 laser energy was slightly reduced. The HCl could act both as a buffer gas to cool the reaction mixture and also as a scavenger of reactive species such as N_3 by reactions of the type $N_3 + HCl \rightarrow HN_3 + Cl$, thus disrupting the reaction chain. Since in this model the induction period represents the time required to achieve a critical N_3 radical density, our observation that HCl lengthens the induction period is reasonable.

Piper *et al.*[24] have recently studied the thermal decomposition of NaN_3 and have observed emission of the $N_2(B\,{}^3\Pi_g - A\,{}^3\Sigma_u^+)$ first-positive bands. They explain their observation by proposing, in addition to Eq. (8), two alternative spin-allowed N_3 recombination routes:

$$2N_3 \rightarrow N_2^*(A\,{}^3\Sigma_u^+) + 2N_2 \ , \tag{9}$$

$$2N_3 \rightarrow N_2^*(B\,{}^3\Pi_g) + 2N_2 \ . \tag{10}$$

The $N_2(B\,{}^3\Pi_g - A\,{}^3\Sigma_u^+)$ emission could thus account for the intrinsic light pulse emitted during the energy releasing, i.e., N_3 recombination, step. In addition, the observed presence of ^3NH could then be accounted for by the reaction[25]

$$N_2^*(B\,{}^3\Pi_g) + HN_3 \rightarrow NH(A\,{}^3\Pi) + 2N_2 \ . \tag{11}$$

The above discussion about the role of N_3 radicals in HN_3 explosions is conjectural and is not based upon any direct evidence we have gathered from TRISP. To detect N_3 by its IR spectrum would require a probe in the vicinity of 2150 cm^{-1} (ν_3 antisymmetric stretch[26]) and considerably more sensitivity than we presently have. A realistic approach towards a more sensitive TRISP apparatus would be to contain the sample with a multipass IR cell.[27] Shifting of the IR probe range to longer wavelengths should be possible with the application of more pump power to the broadband dye laser, or, alternatively, with the utilization of higher p states of the alkali metals.

In summary, we have shown by example how TRISP can be used to probe aspects of the dynamics of fast reactions occurring at relatively high pressures. In the case of laser induced explosions—this would apply also to most combustive processes—TRISP can clearly identify induction periods and phases of rapid energy release, characterizing both with respect to temperature and utilization of reactant material. Spatial inhomogeneities in such reactions, whatever may be the reason for their existence, are also automatically made evident by the technique. In this way, we believe the method is applicable to a wide range of chemical problems.

ACKNOWLEDGMENTS

We would like to thank our colleague, Dr. M. M. T. Loy, for useful suggestions regarding the manuscript and also Dr. A. Hartford of Los Alamos for helpful advice on generation of HN_3.

[1] G. Herzberg, *The Spectra and Structure of Simple Free Radicals* (Cornell University, Ithaca, 1971).
[2] W. R. Ware, "Transient Luminescence Measurements," in

Creation and Detection of the Excited State, edited by A. Lamola (Dekker, New York, 1971), Vol. 1, p. 213.
[3]J. L. Kinsey, Annu. Rev. Phys. Chem. **28**, 349 (1977).
[4]L. J. Bellamy, *The Infrared Spectra of Complex Molecules* (Wiley, New York, 1958).
[5]D. S. Bethune, J. R. Lankard, and P. P. Sorokin, Opt. Lett. **4**, 103 (1979).
[6]D. S. Bethune, J. R. Lankard, M. M. T. Loy, and P. P. Sorokin, IBM J. Res. Dev. **23**, 556 (1979).
[7]J. L. Lyman and R. J. Jensen, J. Phys. Chem. **77**, 883 (1973).
[8]D. S. Bethune, J. R. Lankard, M. M. T. Loy, J. Ors, and P. P. Sorokin, Chem. Phys. Lett. **57**, 479 (1978).
[9]Ph. Avouris, J. Phys. Chem. **84**, 1797 (1980).
[10]B. A. Thrush, Proc. R. Soc. London Ser. A **235**, 143 (1956).
[11]A. E. Douglas and W. J. Jones, Can. J. Phys. **43**, 2216 (1965).
[12]G. Pannetier and A. G. Gaydon, J. Chim. Phys. Phys. Chim. Biol. **48**, 221 (1951).
[13]I. Hajal and J. Combourieu, J. Chim. Phys. Phys. Chim. Biol. **63**, 899 (1966).
[14]N. G. Basov, V. V. Gromov, E. L. Koshelev, E. P. Markin, and A. N. Oraevskii, JETP Lett. **10**, 2 (1969).
[15]M. S. Dzhidzhoev, M. I. Pimenov, V. G. Platonenko, Yu. V. Filippov, and R. V. Khoklov, JETP Lett. **30**, 225 (1970).
[16]A. P. Baronavski, R. G. Miller, and J. R. McDonald, Chem. Phys. **30**, 119 (1978).
[17]A. Hartford, Chem. Phys. Lett. **57**, 352 (1978).
[18]D. C. Hanna, M. A. Yuratich, and D. Cotter, *Nonlinear Optics of Free Atoms and Molecules* (Springer, Berlin, 1979).
[19]D. A. Dows and G. C. Pimentel, J. Chem. Phys. **23**, 1258 (1955).
[20]R. W. B. Pearse and A. G. Gaydon, *The Identification of Molecular Spectra* (Chapman and Hall, London, 1976), 4th edition.
[21]E. H. Eyster, J. Chem. Phys. 8, 135 (1940).
[22]M. Carlotti, G. DiLonardo, G. Galloni, and A. Trombetti, Trans. Faraday Soc. **67**, 2852 (1971).
[23]G. M. Meaburn and S. Gordon, J. Phys. Chem. **72**, 1592 (1968).
[24]L. G. Piper, R. H. Krech, and R. L. Taylor, J. Chem. Phys. **71**, 2099 (1979).
[25]H. Okabe, J. Chem. Phys. **49**, 2726 (1968).
[26]A. D. Yoffe, "The Inorganic Azides," in *Developments in Inorganic Nitrogen Chemistry*, edited by C. B. Colburn (Elsevier, London, 1966).
[27]D. R. Herriott and H. J. Schulte, Appl. Opt. **4**, 883 (1965).